Investigation of the photon statistics of parametric fluorescence in a traveling-wave parametric amplifier by means of self-homodyne tomography

Michael Vasilyev, Sang-Kyung Choi, Prem Kumar, and G. M. D'Ariano*

Department of Electrical and Computer Engineering, Northwestern University, Evanston, Illinois 60208-3118

Received May 21, 1998

Photon-number distributions for parametric fluorescence from a nondegenerate optical parametric amplifier are measured with a novel self-homodyne technique. These distributions exhibit the thermal-state character predicted by theory. However, a difference between the fluorescence gain and the signal gain of the parametric amplifier is observed. We attribute this difference to a change in the signal-beam profile during the traveling-wave pulsed amplification process. © 1998 Optical Society of America

OCIS codes: 270.5290, 190.4410.

Optical homodyne tomography allows one to reconstruct quasi-probability functions if probability distributions $P(X_\phi)$ of the field quadrature $\hat{X}_\phi$ are known for a sufficiently large number of phases ϕ of the local oscillator (LO).[1] This reconstruction method, originally based on a computationally unstable inverse Radon transform, was recently enhanced by a more powerful direct sampling approach.[2] This approach allows one to determine the density-matrix elements ρ_{nm} in the Fock representation by averaging the so-called pattern functions $F_{nm}(X_\phi, \phi)$ over the experimental quadrature outcomes X_ϕ and the LO phase ϕ. The direct sampling method was used to measure the photon statistics of a semiconductor laser,[3] the density matrix of a squeezed state,[4] and, with some modifications, the photon-number correlation between two temporal modes.[5] The procedure of direct sampling is greatly simplified if one is interested only in the photon-number distribution of a quantum state.[3] Since the pattern functions for the diagonal elements ρ_{nn} of the density matrix are independent of ϕ, they can be averaged over quadrature outcomes that are taken at random LO phases, thus eliminating the need for phase locking in the experiment.

The primary focus of optical homodyne tomography is the detection of signatures pertaining to inherently quantum states, e.g., oscillations in the photon-number distribution of a squeezed state. The quest for these signatures, however, puts an extremely severe requirement on the overall quantum efficiency η of photodetection. Interesting quantum features wash out rapidly as η degrades from unity; the washing out occurs more rapidly for states with a larger mean photon number. The requirement of high overall detection efficiency demands not only that the photodetector quantum efficiency be high but also that the homodyne efficiency given by the overlap integral of the signal and the LO modes be as close to unity as possible. To achieve an acceptable level of homodyne efficiency, one has to carefully match the LO and the signal modes.[6] In the case of a nondegenerate optical parametric amplifier (NOPA), a matched LO can be obtained from the same parametric process that generates the signal beam of interest. With type II phase matching, for example, a light beam with polarization at $+45°$ relative to the pump polarization, injected into the NOPA to excite the signal and the idler waves equally, can be utilized at the NOPA output as a matched LO for the detection of squeezed vacuum generated in the $-45°$ polarization direction.[7]

In a similar manner one can utilize a coherent-state beam injected into a parametric amplifier as a LO for homodyning the parametric fluorescence (the signal field) emitted by the NOPA in the same direction and polarization as the injected beam but into modes that are shifted in frequency by, say, $\pm\Omega$.[8] In this case the signal and the LO are matched since they are in the same spatiopolarization mode. Furthermore, such homodyning can be realized with direct detection, since the latter can be considered self-homodyne detection of the amplitude quadrature of a mode that is composed of the two $\pm\Omega$-shifted sidebands. Since the parametric fluorescence has no natural phase reference other than the pump phase, one can easily vary the quadrature phase ϕ by changing the relative phase between the pump and the injected beam.[9] In this Letter we report our results on the measurement of the photon-number distribution of parametric fluorescence from a NOPA, using the self-homodyne technique outlined above.

A schematic of our experimental setup is shown in Fig. 1. The NOPA, consisting of a 5-mm-long KTP crystal, is pumped by the *s*-polarized second harmonic of a *Q*-switched and mode-locked (100-MHz repetition rate) Nd:YAG laser. The NOPA, which is seeded with a *p*-polarized coherent-state signal beam derived from the 1064-nm fundamental output of the same laser, emits pulsed twin beams of light, and only the signal

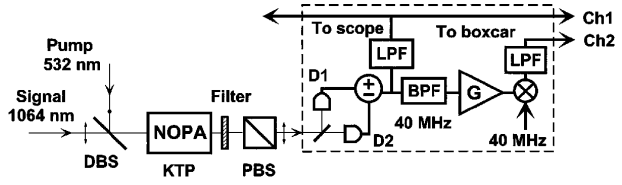

Fig. 1. Schematic of the experimental setup: DBS, dichroic beam splitter; PBS, polarizing beam splitter; LPF's, low-pass filters; BPF, bandpass filter; G, amplifier.

0146-9592/98/171393-03$15.00/0

beam is measured by a balanced set of photodetectors, D1 and D2. The overall quantum efficiency of detection η, including propagation losses from the KTP crystal to the detectors and the quantum efficiency of the photodiodes, is estimated to be 0.8. Low- and high-frequency parts of the sum (or the difference) photocurrent are separated. The peak amplitude of the 5-MHz low-pass-filtered photocurrent is sampled by channel 1 (Ch1) of a boxcar integrator. A 10-MHz-wide band of radio frequencies near $\Omega/2\pi = 40$ MHz is selected by means of a bandpass filter and amplified with a low-noise amplifier. The amplified noise photocurrent is then downconverted to the near-dc region by use of a rf mixer and sampled by channel 2 (Ch2) of the boxcar integrator.

In the process of direct detection, i.e., with the two photodiodes configured to sum the respective photocurrents, the amplified coherent field of the signal beam beats with the $\pm\Omega$-shifted sidebands, thus playing the role of a self-homodyne LO. Assuming the pump phase to be zero, the signal phase to be ϕ, and the rf mixer to be ξ, one can show[9] that the sampled photocurrent in the 10-MHz-wide band near 40 MHz is proportional to the ϕ quadrature, $\hat{X}_\phi = [\exp(-i\phi)\hat{B}^{(\xi)} + \exp(i\phi)\hat{B}^{(\xi)\dagger}]/2$ of a mode $\hat{B}^{(\xi)} = [\exp(i\xi)\hat{b}_{-\Omega} + \exp(-i\xi)\hat{b}_{+\Omega}]/\sqrt{2}$. The detected mode is, therefore, a superposition of the two signal-beam modes that are shifted in frequency by $\pm\Omega$ from the input coherent-state seed. By scanning the phase ϕ of the input signal field with respect to that of the pump field, one can measure any quadrature of the $\hat{B}^{(\xi)}$ mode. In our setup, ϕ is left free to fluctuate randomly; as a result, channel 2 of the boxcar samples a phase-averaged distribution of the noise photocurrent. The proportionality constant between the noise photocurrent and the quadrature fluctuations is eliminated by normalization of the data samples to the shot noise, i.e., to the standard deviation of the data samples that correspond to the vacuum state of $\hat{B}^{(\xi)}$. This standard deviation is obtained independently for each value of the NOPA gain by sampling of the noise in the difference photocurrent of the two balanced photodiodes. The photon-number distribution of the parametric fluorescence in the two-sideband mode $\hat{B}^{(\xi)}$ is then obtained by averaging of the appropriate pattern functions[2] over the experimental phase-averaged quadrature distribution.

The resulting photon-number distributions are shown in Fig. 2 for various values of the NOPA gain. For comparison we also show the theoretical (Bose–Einstein) distributions $P_n = \overline{n}^n/(\overline{n}+1)^{n+1}$ for the thermal states with the same observed mean photon numbers $\overline{n}$, which we measured in each case by averaging the function $2X_\phi{}^2 - 1/2$ over the phase-averaged quadrature distribution. As shown in Fig. 2, there is good agreement between the experimental and the theoretical distributions, which verifies that the parametric fluorescence from our NOPA exhibits the statistical character of the thermal state.

In our experiment the parametric fluorescence takes place only within the duration of the mode-locked pulses underneath the Q-switch envelope of the pump field. By passing the noise photocurrent through a 10-MHz bandpass filter, we essentially average the fluorescence over several mode-locked pulses. Our boxcar, which samples the noise at the peak of the Q-switch temporal envelope, thus measures the fluorescence contribution of only a few mode-locked pulses near the peak of the Q-switch envelope. Therefore the mean photon number $\overline{n}$ observed in our experiment can be related to the optical power P of the parametric fluorescence that is measured in the spectral bandwidth of $\Delta\omega/2\pi = 10$ MHz at the peak of the Q-switch temporal envelope, i.e., $P = \overline{n}h\omega\Delta\omega/(2\pi\eta)$.

In Fig. 3 we plot the effective gain in the two-sideband mode $\hat{B}^{(\xi)}$, $g_{\text{eff}} = (\overline{n}/\eta + 1)$, determined from experimental measurements of the noise, versus the mean-power gain g_p determined from measurements of the low-pass-filtered photocurrent. Although the two gains are expected to be the same for cw beams with plane-wave spatial properties (dashed curve), they differ considerably in our experiment. We believe that this is so because of the narrowing of the signal width in both the spatial and the temporal domains as a consequence of the traveling-wave pulsed amplification process.[10] We illustrate this effect by taking only the spatial narrowing into account. In this case the measured mean-power gain is given by $g_p = [\iint g(\boldsymbol{\rho})|e_{\text{in}}(\boldsymbol{\rho})|^2\,d\boldsymbol{\rho}]/[\iint |e_{\text{in}}(\boldsymbol{\rho})|^2\,d\boldsymbol{\rho}]$. Here $g(\boldsymbol{\rho}) = \cosh^2[\beta e_p(\boldsymbol{\rho})]$ is the spatial profile of the gain, $e_{\text{in}}(\boldsymbol{\rho})$ is the amplitude of the input signal field, $e_p(\boldsymbol{\rho})$ is the amplitude of the pump field, β is proportional to the effective nonlinearity times the NOPA length, and the integration is over the transverse spatial coordinates defined by the vector $\boldsymbol{\rho}$. Assuming that the quadrature $\hat{X}_\phi$ of parametric fluorescence exhibits only point-to-point correlations, i.e., $\langle \hat{X}_\phi(\boldsymbol{\rho})\hat{X}_\phi(\boldsymbol{\rho}')\rangle = \delta(\boldsymbol{\rho} - \boldsymbol{\rho}') \times (2g - 1)/4$, the

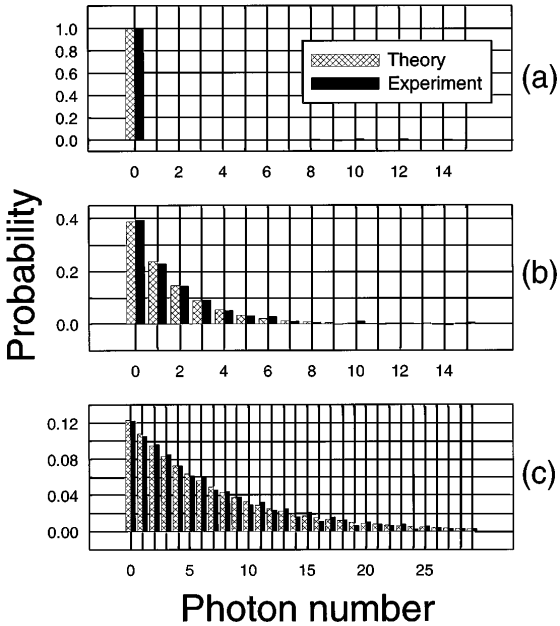

Fig. 2. Photon-number distributions for mean-power gains of (a) $g_p = 1$ (vacuum state), (b) $g_p = 2$, and (c) $g_p = 4$. Theoretical distributions for the same mean photon numbers are also plotted. The experimental distributions in (a) and (b) are reconstructed from 80,000 samples, and that in (c) is from 320,000 samples.

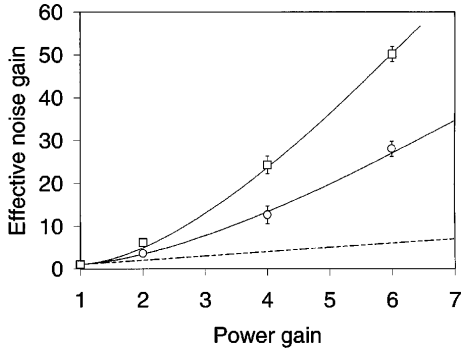

Fig. 3. Effective noise gain versus mean-power gain. Signal spot sizes are 55 μm (squares) and 40 μm (circles). The pump spot size is 28 μm in both cases. Solid curves, results of numerical calculations; dashed curve, result expected for a cw plane wave.

effective gain obtained from the noise measurements is given by $g_{\mathrm{eff}} = [\iint g^2(\boldsymbol{\rho})\,|e_{\mathrm{in}}(\boldsymbol{\rho})|^2\,\mathrm{d}\boldsymbol{\rho}]/[\iint g(\boldsymbol{\rho})\,|e_{\mathrm{in}}(\boldsymbol{\rho})|^2\,\mathrm{d}\boldsymbol{\rho}]$, where the denominator represents the coherent-state noise level of the self-homodyne LO. For Gaussian beams the gain profile $g(\boldsymbol{\rho})$ narrows with respect to the input signal profile $|e_{\mathrm{in}}(\boldsymbol{\rho})|^2$ with increasing pump power. The overlap between $g(\boldsymbol{\rho})$ and $|e_{\mathrm{in}}(\boldsymbol{\rho})|^2$ in the expression for g_p becomes worse than the overlap between $g(\boldsymbol{\rho})$ and the self-homodyne LO profile $g(\boldsymbol{\rho})\,|e_{\mathrm{in}}(\boldsymbol{\rho})|^2$ in the expression for g_{eff}. As a result the gain inferred from the noise measurements is higher than the observed power gain. A similar, although one-dimensional, effect also occurs in the time domain.

For the two sets of data presented in Fig. 3 the pump spot size was 28 μm and the signal spot sizes were 55 and 40 μm. The widths of the Q-switched envelopes (mode-locked pulses) were 205 ns (120 ps) for the signal beam and 145 ns (85 ps) for the pump beam. The numerically calculated g_{eff} for these parameters, with the effects of both the spatial and temporal narrowing taken into account, are shown in Fig. 3 by the solid curves, which indicate good agreement with the measured data.

Note that, for tightly focused beams or for high parametric gains, the assumption of pointwise quadrature correlation used in our numerical model may not be justified because of the finite spatial bandwidth of the OPA, which in turn is determined by the phase-matching condition. In that case a more precise calculation of the effective noise gain versus mean-power gain would be needed. However, in our present setup we believe that the spatial profiles of both the pump and the amplified signal beams are well within the OPA spatial bandwidth, and hence the assumption of pointwise correlation is valid. By comparing the data sets for the two different signal spot sizes, we conclude that the difference between the mean-power and the noise gains decreases as the pump spot size increases relative to the signal spot size. One can eliminate this gain difference that is due to the signal spatial profile narrowing by choosing the pump spot size to be sufficiently large compared with the signal spot size. The effect of signal profile narrowing in the time domain can in principle be avoided by use of pump pulses that are considerably longer than the signal pulses, although this is not usually an option in typical parametric amplification experiments.

The success of the self-homodyne approach in measuring the photon statistics of parametric fluorescence suggests that one can also use it to determine the joint photon-number distribution of the twin beams produced by the NOPA. For measuring such a joint distribution, we propose adding a coherent-state seed to the input of the NOPA's idler mode and jointly sampling the amplified signal and idler photocurrent noises. Although the NOPA gain in this configuration is phase sensitive, one can use the value of the gain estimated from the low-pass-filtered measurements to find the joint quadrature fluctuations from the photocurrent-noise data. Also, the LO phases at the NOPA output will be correlated owing to phase-sensitive amplification, which can be corrected by averaging of the experimental outcomes taken at different phases with an appropriate weight function, which turns out to be the reciprocal of the phase-sensitive gain.[9] The discrepancy between the mean-power and the noise gains, as investigated above, would be a detrimental factor in such a reconstruction method. Avoiding or minimizing such a discrepancy is possible by use of a pump beam whose intensity stays approximately constant across the signal-beam spatiotemporal profile.

The authors thank D. Levandovsky for useful discussions and M. L. Marable for help at the initial stage of the experiment. This work was supported in part by the U.S. Office of Naval Research.

*Permanent address, Università di Pavia, via Bassi 6, I 27100 Pavia, Italy.

References

1. D. T. Smithey, M. Beck, M. G. Raymer, and A. Faridani, Phys. Rev. Lett. **70,** 1244 (1993); G. Breitenbach, T. Müller, S. F. Pereira, J.-Ph. Poizat, S. Schiller, and J. Mlynek, J. Opt. Soc. Am. B **12,** 2304 (1995).
2. G. M. D'Ariano, C. Macchiavello, and M. G. A. Paris, Phys. Rev. A **50,** 4298 (1994); G. M. D'Ariano, U. Leonhardt, and H. Paul, Phys. Rev. A **52,** R1801 (1995); U. Leonhardt, M. Munroe, T. Kiss, Th. Richter, and M. G. Raymer, Opt. Commun. **127,** 144 (1996).
3. M. Munroe, D. Boggavarapu, M. E. Anderson, and M. G. Raymer, Phys. Rev. A **52,** R924 (1995).
4. S. Schiller, G. Breitenbach, S. F. Pereira, T. Müller, and J. Mlynek, Phys. Rev. Lett. **77,** 2933 (1996).
5. M. G. Raymer, D. F. McAlister, and U. Leonhardt, Phys. Rev. A **54,** 2397 (1996); D. F. McAlister and M. G. Raymer, Phys. Rev. A **55,** R1609 (1997).
6. J. H. Shapiro and A. Shakeel, J. Opt. Soc. Am. B **14,** 232 (1997).
7. C. Kim and P. Kumar, Phys. Rev. Lett. **73,** 1605 (1994).
8. M. V. Vasilyev, M. L. Marable, S.-K. Choi, P. Kumar, and G. M. D'Ariano, in *Quantum Electronics and Laser Science Conference*, Vol. 12 of 1997 OSA Technical Digest Series (Optical Society of America, Washington, D.C., 1997), pp. 95–96.
9. G. M. D'Ariano, M. Vasilyev, and P. Kumar, Phys. Rev. A **58,** 636 (1998).
10. S.-K. Choi, R.-D. Li, C. Kim, and P. Kumar, J. Opt. Soc. Am. B **14,** 1564 (1997).